molecular pharmaceutics

Article

pubs.acs.org/molecularpharmaceutics

Radioiodinated Folic Acid Conjugates: Evaluation of a Valuable Concept To Improve Tumor-to-Background Contrast

Josefine Reber,[†] Harriet Struthers,[‡] Thomas Betzel,[‡] Alexander Hohn,[†] Roger Schibli,[†,‡] and Cristina Müller*[,†]

[†]Center for Radiopharmaceutical Sciences ETH-PSI-USZ, Paul Scherrer Institute, Villigen-PSI, Switzerland

[‡]Department of Chemistry and Applied Biosciences, ETH Zurich, Zurich, Switzerland

Supporting Information

ABSTRACT: Folic acid radioconjugates can be used for targeting folate receptor positive (FR^+) tumors. However, the high renal uptake of radiofolates is a drawback of this strategy, particularly with respect to a therapeutic application due to the risk of damage to the kidneys by particle radiation. The goal of this study was to develop and evaluate radioiodinated folate conjugates as a novel class of folate-based radiopharmaceuticals potentially suitable for therapeutic application. Two different folic acid conjugates, tyrosine-folate (**1**) and tyrosine-click-folate (**3**), were synthesized and radioiodinated using the Iodogen method resulting in [^{125}I]-**2** and [$^{125/131}$I]-**4**. Both radiofolates were highly stable in mouse and human plasma. Determination of FR binding affinities using ^{3}H-folic acid and FR^+ KB tumor cells revealed affinities in the nanomolar range for **2** and **4**. The cell uptake of [^{125}I]-**2** and [$^{125/131}$I]-**4** proved to be FR specific as it was blocked by the coincubation of folic acid. 3-(4,5-Dimethylthiazol-2-yl)-2,5-diphenyltetrazolium bromide (MTT) *in vitro* assays were employed for the determination of tumor cell viability upon exposure to [^{131}I]-**4**. Compared to untreated control cells, significantly reduced cell viability was observed for FR^+ cancer cells (KB, IGROV-1, SKOV-3), while FR^- cells (PC-3) were not affected. Biodistribution studies performed in tumor bearing nude mice showed the specific accumulation of both radiofolates in KB tumor xenografts ([^{125}I]-**2**: 3.43 ± 0.28% ID/g; [^{125}I]-**4**: 2.28 ± 0.46% ID/g, 4 h p.i.) and increasing tumor-to-kidney ratios over time. The further improvement of the tumor-to-background contrast was achieved by preinjection of the mice with pemetrexed allowing excellent imaging via single-photon emission computed tomography (SPECT/CT). These findings confirmed the hypothesis that the application of radioiodinated folate conjugates may be a valuable concept to improve tumor-to-background contrast. The inhibitory effect of [^{131}I]-**4** on FR^+ cancer cells *in vitro* indicates the potential of this class of radiofolates for therapeutic application.

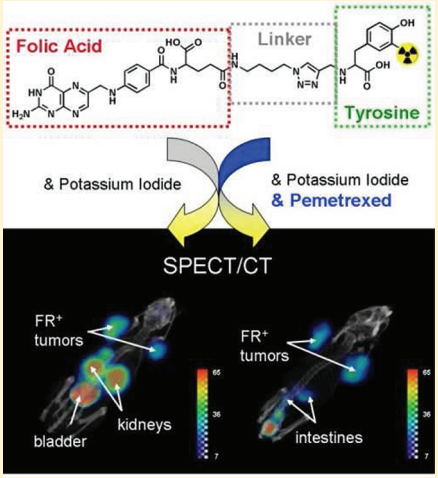

KEYWORDS: *folate receptor, tyrosine-folate, iodine, SPECT/CT, radionuclide therapy*

INTRODUCTION

The folate receptor (FR) emerged as a valuable tumor marker because of its overexpression in a variety of cancer types and the fact that it can be targeted by the vitamin folic acid.[1−4] Folate-based radiopharmaceuticals have attracted significant interest for nuclear imaging of cancer with single-photon emission computed tomography (SPECT; ^{99m}Tc, ^{111}In, ^{67}Ga) and positron emission tomography (PET; ^{68}Ga, ^{18}F) (reviewed in refs 5−7). However, the FR is also expressed on the luminal side of proximal tubule cells in the kidneys and thus accessible to filtered (radio)folates.[8−10] The result is a high kidney accumulation of folate radiopharmaceuticals and hence low tumor-to-kidney ratios (~0.1).[11] Therefore, there is an inherent risk of damage to the kidneys by application of therapeutic radiofolates. Nevertheless, this treatment strategy is attractive in view of the large number of patients who could benefit from it. Thus, establishing effective strategies to improve the tumor-to-kidney ratio of radiofolates is of paramount interest. We have previously investigated the application of radiofolates in combination with the chemotherapeutic antifolate pemetrexed (PMX), which was able to improve the tumor-to-kidney ratios significantly.[12−14] The application of PMX in combination with therapeutic radiofolates would be particularly beneficial if it had an additional or synergistic tumor growth inhibitory effect.

Radioiodination of tyrosine residues is a common strategy for efficient radiolabeling of proteins and peptides, demonstrated in numerous studies of small and large biomolecules. The instability of radioiodinated tyrosine constructs as a consequence of *in vivo* deiodination is generally regarded as a disadvantage for radiopharmaceutical applications. However, in a recent study, Zardi and co-workers showed that the tumor-to-

Received: October 8, 2011
Revised: February 12, 2012
Accepted: April 5, 2012
Published: April 17, 2012

kidney ratios of the radioiodinated antibody fragment L19 was significantly increased over time (~0.36, 1 h p.i.; ~ 6.71, 24 h p.i.).[15] In contrast, the same antibody fragment radiolabeled with ^{99m}Tc showed a very low tumor-to-kidney ratio of ~0.1 at all time points after injection.[16] Thus, we hypothesized that radioiodinated folate conjugates would exhibit favorable properties, similar to those found with the radioiodinated antibody fragment L19. The partial deiodination of radioiodinated folate conjugates might result in a quick clearance of released iodide via kidneys and thus lead to improved tumor-to-kidney ratios. The design of radioiodinated folic acid conjugates as an alternative to folate-linked chelates for stable coordination of radiometals could be an effective strategy to achieve an improved tumor-to-background contrast.

Another advantage of radioiodinated folate conjugates is the opportunity to employ a range of iodine radioisotopes suitable for imaging and therapeutic purposes. The long-lived radioisotope iodine-125 ($T_{1/2}$ = 59.4 d, E_γ = 35.5 keV (6.7%), Auger-e$^-$) is usually favored for preclinical *in vitro* and *in vivo* studies including small-animal imaging. For clinical applications, the radiolabeling of biomolecules with iodine-123 ($T_{1/2}$ = 13.2 h, E_γ = 159 keV (83%)) or iodine-124 ($T_{1/2}$ = 4.18 d, I_{β^+} = 23%, E_{β^+} (max) = 2140 keV) is useful for SPECT and PET imaging and can be regarded as diagnostic and dosimetric substitutes for the therapeutic counterpart iodine-131 ($T_{1/2}$ = 8.03 d, I_{β^-} = 100%, E_{β^-} (average) = 182 keV; E_γ = 365 keV (82%)).

The goal of this study was to evaluate the proposed concept of partial deiodination of radioiodinated folate conjugates as a method to improve the tumor-to-kidney ratio of radiofolates. We therefore prepared two structurally different folate conjugates, the tyrosine-folate (**1**) and the tyrosine-click-folate (**3**). The ^{125}I-radioiodinated folate tracers [^{125}I]-**2** and [^{125}I]-**4** were evaluated *in vitro* using FR positive KB tumor cells. To assess the tissue distribution of radioactivity, animal experiments including SPECT/CT imaging studies were performed. The novel radiofolates were also tested in combination with PMX. The second objective of this study was to investigate the cytotoxic effect of the ^{131}I-radioiodinated tyrosine-click-folate ([^{131}I]-**4**) *in vitro* by employing a standard cell viability assay. By application of FR targeted *in vitro* therapy using the particle-emitting radioiodine-131 in combination with PMX, a potentially enhanced effect of these two treatment modalities was assessed using FR positive and FR negative cancer cell lines.

EXPERIMENTAL SECTION

Radioiodination. The synthesis of compounds **1** to **4** (Figure 1) is reported in the Supporting Information (SI, section 1, Figures S1−S3, Table S1). Compounds **1** and **3** were radiolabeled with [^{125}I]iodine and [^{131}I]iodine isotopes obtained from Perkin-Elmer (Waltham, MA, USA). Specific activities were indicated as ~629 GBq/mg (~ 78.6 MBq/nmol) for [^{125}I]iodine and >185 GBq/mg (>24.2 MBq/nmol) for [^{131}I]iodine. Radioiodination was performed using the Iodogen method as previously described.[17] In brief, sodium radioiodide (^{125}I: up to 60 MBq; ^{131}I: up to 45 MBq) dissolved in tris(hydroxymethyl)aminomethane (TRIS) buffer pH 7.6 was added to an Iodogen-coated (0.05 μg) reaction vial. The oxidation reaction was allowed to proceed for 5 min at room temperature. The solution containing the activated ^{125}I or ^{131}I was removed from the insoluble oxidizing agent and transferred to a reaction vial containing 10−30 μL of the folate precursor **1** or **3** (1 mM), respectively. The labeling procedure was performed at room temperature for 5 min with [^{131}I]iodine or 15 min with [^{125}I]iodine. Quality control was performed by high-performance liquid chromatography (HPLC) as reported in detail in the SI (section 1, Figure S3). The radioiodinated compounds [^{125}I]-**2** (retention time (R_t) ≈ 14.4 min) and [$^{125/131}$I]-**4** (R_t ≈ 15.7 min) were separated from traces of free iodide (R_t ≈ 2.9 min) and cold precursor **1** (R_t ≈ 12.4 min) or **3** (R_t ≈ 13.9 min) by means of HPLC using the same method as established for analysis. For *in vitro* and *in vivo* experiments methanol in the collected HPLC fraction was evaporated, and the radiofolate solution was diluted with phosphate-buffered saline (PBS) at pH 7.4. The determination of the octanol/PBS distribution coefficient (log *D* value) is reported in the SI (section 2).

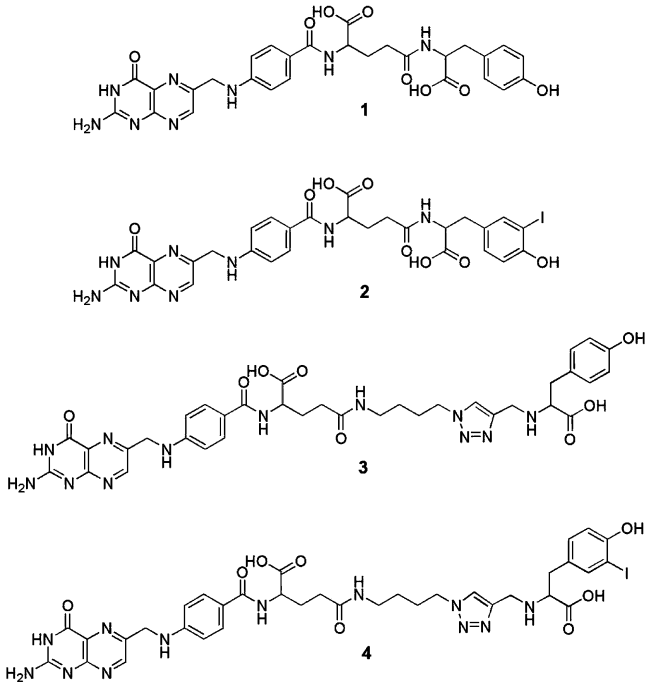

Figure 1. Chemical structures of folate conjugates **1**−**4**.

Stability Experiments. The stabilities of [^{125}I]-**2** and [^{125}I]-**4** were determined in mouse and human plasma. HPLC-purified radiofolates (~2.0 MBq, 50 μL) were mixed with 250 μL of mouse or human plasma and incubated at 37 °C. Aliquots were taken for analysis at defined time points after incubation (0, 4, 24, 48, 72, and 168 h). Plasma samples of 50 μL were precipitated with 200 μL of methanol and centrifuged twice before injection into the HPLC. *In vitro* studies for the determination of the metabolic stability were performed using murine liver microsomes and are reported in the SI (section 3, Figure S4). *In vivo* studies in mice performed to determine potential metabolites and/or deiodination are reported in the SI (section 4, Table S2).

Cell Culture. KB cells (human cervix carcinoma cell line, ACC-136) and PC-3 (human prostate carcinoma cell line, ACC-465) were purchased from the German Collection of Microorganisms and Cell Cultures (DSMZ, Braunschweig, Germany). IGROV-1 cells (human ovarian carcinoma cell line) were a kind gift from Dr. Gerrit Jansen (Department of Rheumatology, VU University Medical Center, Amesterdam, The Netherlands). SKOV-3 i.p. cells (human ovarian adenocarcinoma cancer cell line, herein referred as to SKOV-3[18]) were kindly provided by Dr. Ilse Novak-Hofer

(Center for Radiopharmaceutical Sciences ETH-PSI-USZ, Paul Scherrer Institute, Switzerland). KB cells are known to express the FR at very high levels, whereas IGORV-1 and SKOV-3 cells express the FR at lower levels.[1,19,20] PC-3 cells that do not express the FR were used as a negative control.[21] The cells were cultured as monolayers at 37 °C in a humidified atmosphere containing 5% CO_2. PC-3 cells were cultured in Roswell Park Memorial Institute (RPMI) 1640 medium (Amimed, Bioconcept, Switzerland). Importantly, KB, IGROV-1, and SKOV-3 cells were cultured in a folate free RPMI cell culture medium referred to as FFRPMI (without folic acid, vitamin B_{12}, and phenol red; Cell Culture Technologies GmbH, Gravesano/Lugano, Switzerland). FFRPMI and RPMI media were supplemented with 10% heat-inactivated fetal calf serum, L-glutamine, and antibiotics. Routine culture treatment was performed twice a week.

Cell Uptake and Internalization. KB cells were seeded in 12-well plates to grow overnight (~700 000 cells in 2 mL FFRPMI medium/well). HPLC purified compounds [^{125}I]-**2** and [^{125}I]-**4** (~0.04 MBq, ~0.5 pmol) were added to each well. In some cases cells were incubated with excess folic acid to block FRs on the surface of KB cells. After incubation at 37 °C for different time periods (5, 15, 30, 60, 120, and 240 min), the cells were washed three times with PBS to determine total radiofolate uptake. To assess the internalized fraction of radiofolate, KB cells were additionally washed with a stripping buffer (aqueous solution of 0.1 M acetic acid and 0.15 M NaCl, pH 3)[22] to release FR bound radiofolates from the cell surface.[3] Cell lysis was accomplished by the addition of 1 mL of 1 N NaOH to each well. The cell suspensions were transferred to 4 mL tubes, and each sample was counted in a γ-counter. After homogenization by vortex, the protein concentration was determined for each sample using a Micro BCA Protein Assay kit. The measured radioactivity was standardized to the average content of 0.3 mg of protein in a single well.

***In Vitro* Binding Affinity Assays.** Binding assays with nonradioactive reference compounds **2** and **4** were performed with KB tumor cells suspended in PBS at pH 7.4 (7000 cells/240 μL per Eppendorf tube). The cells were incubated in triplicate with ^{3}H-folic acid (10 μL, 0.84 nM) and increasing concentrations of the nonradioactive reference compound (5.0×10^{-7} to 5.0×10^{-12} M in 250 μL of PBS at pH 7.4) on a shaker at 4 °C for 30 min. Nonspecific binding was determined in the presence of excess folic acid (10^{-3} M). After incubation, Eppendorf tubes containing the cell suspensions were centrifuged at 4 °C for 5 min, and the supernatant was removed. By addition of 0.5 mL of NaOH (1 N) the cell pellets were lysed and transferred into scintillation tubes containing 5 mL of scintillation cocktail (Ultima Gold; Perkin-Elmer). The radioactivity was measured using a liquid scintillation analyzer (Tri-Carb 1900 TR, Packard), and an inhibitory concentration of 50% was determined from displacement curves using *GraphPad Prism* (version 5.01) software. Relative affinities were defined as the inverse molar ratio of test compounds required to displace 50% of ^{3}H-folic acid, and the relative FR affinity of folic acid was set to 1.

MTT Assay. The inhibition of cell growth was evaluated using a 3-(4,5-dimethylthiazol-2-yl)-2,5-diphenyltetrazolium bromide (MTT) assays. KB, IGROV-1, SKOV-3, and PC-3 cells were harvested and seeded in 96-well plates at 2.5×10^3 cells per well in a final volume of 200 μL of FFRPMI medium (KB, IGROV-1, and SKOV-3) or RPMI medium (PC-3) with supplements. After 24 h incubation for cell adhesion, the medium was removed, and the cells were incubated at 37 °C with 200 μL of FFRPMI medium (without supplements) containing [^{131}I]-**4** (0.50 MBq/mL, corresponding to 20 nM folate tracer) alone or in combination with excess folic acid (200 nM) to block FRs. To determine the amount of radiofolate [^{131}I]-**4** necessary to reduce cell viability to 50% of untreated cells, KB, IGROV-1 and SKOV-3 cells were incubated for 4 h at 37 °C with 200 μL of FFRPMI medium (without supplements) containing [^{131}I]-**4** (10.0, 5.0, 1.0, 0.5, 0.1, 0.05, and 0.01 MBq/mL). For the investigation of a potential effect of PMX (Alimta, LY231514; Eli Lilly, Bad Homburg, Germany) on cell viability, KB cells were incubated with [^{131}I]-**4** (0.01 MBq/mL) or PMX (1 μM) alone or with a combination of these two agents for 4 or 24 h at 37 °C. Cell incubation with FFRPMI medium only was performed as a control experiment. After incubation, the cells were washed with 200 μL of PBS, and 200 μL of supplemented FFRPMI or RPMI medium was added. Four days later, 30 μL of a filtered MTT solution in PBS (5 mg/mL) was added to each well, and incubation was continued for an additional 4 h at 37 °C. The medium was removed, and the dark-violet formazan crystals were dissolved in 200 μL of dimethyl sulfoxide (DMSO). The absorbance was determined at 560 nm using a microplate reader (Victor X3, Perkin-Elmer). To quantify cell viability, the ratio of the absorbance of the samples to the absorbance of control cell samples (= 100% viability) was calculated.

Biodistribution Studies. *In vivo* experiments were approved by the local veterinarian department and conducted in accordance with the Swiss law of animal protection. Six- to eight-week-old female, athymic nude mice (CD-1 Foxn-1/nu) were purchased from Charles River Laboratories (Sulzfeld, Germany). The animals were fed with a folate deficient rodent diet (Harlan Laboratories, Indianapolis, IN, U.S.) starting 5 days prior to tumor cell inoculation.[23] Mice were inoculated with KB cells (5×10^6 cells in 100 μL of PBS) into the subcutis of each shoulder. Animal experiments were performed approximately 14 days after tumor cell inoculation. Biodistribution studies were performed in triplicate. Radiofolates [^{125}I]-**2** and [^{125}I]-**4** were diluted in PBS pH 7.4 for immediate administration via a lateral tail vein (0.2 MBq, 2.5 pmol, 100 μL per mouse). Potassium iodide was dissolved in PBS and injected intraperitoneally (4 mg, 200 μL), 1 h prior to the radioactivity. Blocking experiments were performed 4 h after injection, with mice coinjected with excess folic acid dissolved in PBS (100 μg, 100 μL). The animals were sacrificed at 1, 4, or 24 h after administration of the radiofolate. Selected tissues and organs were collected, weighed, and counted for radioactivity in a γ-counter. The results were recorded as the percentage of the injected dose per gram of tissue weight [% ID/g]. Biodistribution studies performed with [^{125}I]-**4** in combination with preinjected PMX are reported in the SI (section 5, Figure S5).

Statistical analyses were performed by using a *t*-test (*Microsoft Excel* software). All analyses were two-tailed and considered as type 3 (two sample unequal variance). A *p*-value of <0.05 was considered statistically significant.

SPECT/CT Imaging Studies and *ex Vivo* Autoradiography. Imaging experiments were performed using an X-SPECT system (Gamma Medica Inc., Northridge, CA, USA) with a small animal single-head SPECT/CT device. Radiofolate [^{125}I]-**4** (~5.0 MBq; ~64 pmol) was injected into a lateral tail vein of KB tumor-bearing nude mice. PMX was diluted with NaCl to 0.9% according to the instructions of the manufacturer

and injected into a lateral tail vein (400 μg, 100 μL), 1 h before the radiotracer.[12,13] SPECT scans of 60 min duration were performed approximately 24 h after injection of the radiotracer followed by CTs. SPECT data were collected and reconstructed using the software *LumaGEM* (version 5.407; Gamma Medica Inc.). CT data were acquired with an X-ray CT system (Gamma Medica Inc.) and reconstructed with the software *COBRA* (version 4.5.1). The fusion of SPECT and CT data was performed with *IDL Virtual Machine* (version 6.0) software. Images were generated by the software *Amira* (version 4.0.1). *Ex vivo* autoradiography studies are reported in the SI (section 6).

RESULTS

Synthesis and Radioiodination. Compounds **1**−**4** are shown in Figure 1. The organic synthesis and chemical characterization are reported in the SI (Figures S1 and S2, Table S1). Radioiodination of folate compounds **1** and **3** was obtained with $^{125/131}$I, in a radiochemical yield of >97%. The shift to longer HPLC retention times of radiolabeled compounds [^{125}I]-**2** and [$^{125/131}$I]-**4** enabled their separation from the unlabeled precursors **1** and **3** to obtain the highest possible specific activities corresponding to the specific activities of the radionuclides (~629 GBq/mg, i.e., ~78.6 MBq/nmol for ^{125}I and >185 GBq/mg, i.e., >24.2 MBq/nmol for ^{131}I; SI, Figure S3).

***In Vitro* Evaluation.** Cell uptake studies showed ^{125}I-tyrosine-folate ([^{125}I]-**2**) and ^{125}I-tyrosine-click-folate ([^{125}I]-**4**) had similar characteristics and were comparable to previously evaluated radiofolates.[24] The maximal amount of uptake was reached after an incubation time of about 90−120 min at 37 °C. The internalized fraction of both radiofolates accounted for 25−30% of total cell uptake (sum of FR bound radiofolate on the cell surface and internalized fraction). Co-incubation of excess folic acid resulted in an inhibition of radiofolate uptake for both [^{125}I]-**2** and [^{125}I]-**4** to less than 0.1% of the total added radioactivity (Figure 2).

Relative binding affinities were determined using a competition assay with ^{3}H-folic acid and the nonradioactive reference compounds **2** and **4**. The binding affinity of folic acid was set to 1.0. A relative affinity value of 1.0 implies that the test compound has an affinity for the FR equal to that of folic acid. Likewise, values lower than 1.0 reflect a weaker affinity, and values higher than 1.0 reflect a stronger affinity.[25,26] For our test compounds the determination of binding affinities resulted in relative values of 0.78 for I-tyrosine-folate (**2**) and 0.67 for I-tyrosine-click-folate (**4**).

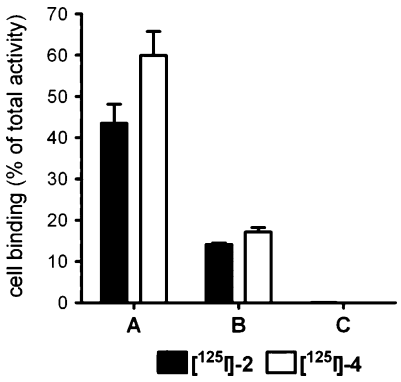

Figure 2. Cell binding (A) and internalization (B) of ^{125}I-labeled tyrosine-folate ([^{125}I]-**2**) and tyrosine-click-folate ([^{125}I]-**4**) in KB cells after an incubation time of 120 min at 37 °C. Blockade (C) of FR by coincubation with excess folic acid resulted in an uptake of less than 1%.

In vitro stability experiments were performed in both mouse and human plasma. Within the time period of investigation (7 days), HPLC analysis of the collected and precipitated plasma samples showed always only one single peak with an integrated area of 100% and a retention time that corresponded to the radioiodinated folate conjugates ([^{125}I]-**2** or [^{125}I]-**4**). Thus, no signs of deiodination or decomposition of the radioiodinated compounds [^{125}I]-**2** and [^{125}I]-**4** was determined. In addition, potential deiodination of [^{125}I]-**2** or [^{125}I]-**4**) was investigated using murine liver microsomes. However, in contrast to [^{125}I]iodo-L-tyrosine which was almost completely deiodinated within 30 min, the deiodination of the radiofolates ([^{125}I]-**2** or [^{125}I]-**4**) was not determined over a time period of 24 h (SI, section 3, Figure S4).

***In Vitro* Cell Viability Study.** An MTT assay was employed to test the effect of the ^{131}I-radiolabled folate conjugate ([^{131}I]-**4**, Figure 3). In the absence of folic acid, the incubation of FR-positive cells with ^{131}I-tyrosine-click-folate ([^{131}I]-**4**, 5 MBq/mL) reduced viability of KB, IGROV-1, and SKOV-3 cells to 4.5%, 15.3%, and 27.4% of untreated control cells (Figure 3A). However, if the cells were coincubated with excess folic acid to block FRs, cell viability was not affected by application of radiofolate [^{131}I]-**4** at the same radioactivity concentrations. In addition, no inhibition of cell viability was observed with the same amount of [^{131}I]-**4** in control experiments performed with FR negative PC-3 cells (Figure 3A). The determination of the amount of [^{131}I]-**4** necessary to reduce cell viability of KB, IGROV-1, and SKOV-3 cells to 50% of untreated control cells revealed radioactivity concentrations of 0.39 ± 0.03 MBq/mL, 0.95 ± 0.05 MBq/mL, and 1.22 ± 0.09 MBq/mL, respectively (Figure 3B).

The incubation of KB cells with PMX (1 μM) for 4 h and 24 h, respectively, reduced tumor cell viability to 80% and 50% of untreated controls (Figure 4). The application of the [^{131}I]-**4** at a concentration of 0.01 MBq/mL did not affect tumor cell viability if applied as a single agent for 4 h. However, if this radioactivity concentration was applied in combination with PMX (1 μM), it resulted in an enhanced inhibitory effect, decreasing cell viability to 72% (after 4 h) and 23% (after 24 h) compared with untreated controls.

Biodistribution Studies. Biodistribution data for [^{125}I]-**2** and [^{125}I]-**4** are shown in Table 1. Both radiotracers accumulated in FR positive KB tumor xenografts and in the kidneys. The tumor uptake of ^{125}I-tyrosine-folate ([^{125}I]-**2**: 4.42 ± 0.66% ID/g) was higher than the uptake of ^{125}I-tyrosine-click-folate ([^{125}I]-**4**: 2.36 ± 0.05% ID/g) at 1 h after injection (p = 0.02). However, tumor retention over time was superior for [^{125}I]-**4** (1.92 ± 0.24% ID/g, 24 h p.i.) compared to [^{125}I]-**2** (1.25 ± 0.18% ID/g, 24 h p.i.). The reduction of the tumor uptake after coinjection of excess folic acid (4 h p.i.) was pronounced in the case of [^{125}I]-**4** (<2% of control values), whereas in the case of [^{125}I]-**2** tumor uptake could only be reduced to 48% of the control values.

The renal accumulation of radioactivity was high (~19% ID/g) 1 h after injection for both radiofolates. However, 4 h after injection there was a significant difference (p = 0.03) between [^{125}I]-**2** (9.80 ± 1.67% ID/g) and [^{125}I]-**4** (16.44 ± 2.64% ID/g). At 24 h after injection this difference was even more pronounced ([^{125}I]-**2**: 0.85 ± 0.06% ID/g vs [^{125}I]-**4**: 7.10 ±

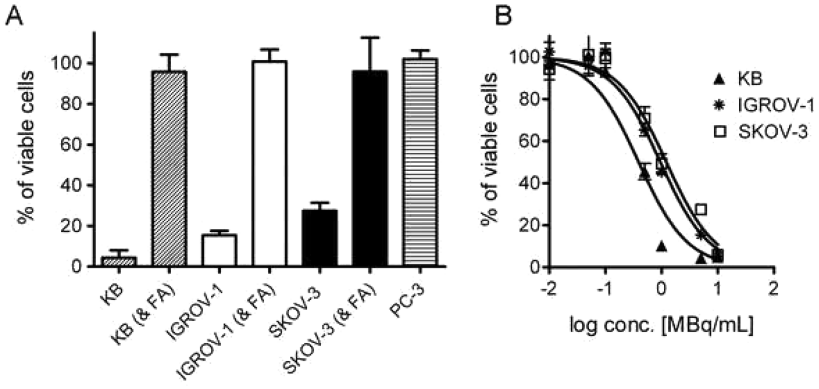

Figure 3. (A) Effects of ^{131}I-tyrosine-click-folate [^{131}I]-**4** (5 MBq/mL, corresponding to 200 nM folate conjugate) on FR-positive KB, IGROV-1, and SKOV-3 cells and FR-negative PC-3 cells after incubation for 4 h at 37 °C in the presence and absence of excess folic acid (FA). (B) Determination of the concentration of [^{131}I]-**4** (MBq/mL) which is necessary to reduce cell viability to 50% of untreated control cells (KB: 0.39 ± 0.03 MBq/mL; IGROV-1: 0.95 ± 0.05 MBq/mL; and SKOV-3: 1.22 ± 0.09 MBq/mL).

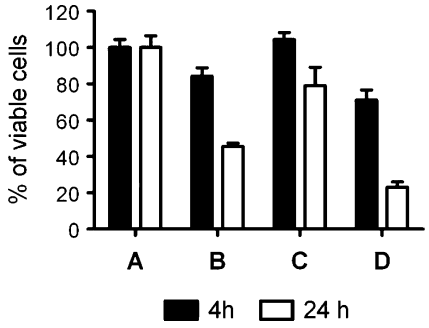

Figure 4. Percentage of viable KB cells after incubation for 4 and 24 h at 37 °C (A) with culture medium only (= 100%, control experiment), (B) with PMX (1 μM), (C) with ^{131}I-tyrosine-click-folate ([^{131}I]-**4**: 0.01 MBq/mL), and (D) with the combination of PMX and [^{131}I]-**4**.

1.44% ID/g; p = 0.02). The application of [^{125}I]-**4** after preinjection of PMX resulted in a significantly reduced uptake of radioactivity in the kidneys, while uptake in the tumor xenografts was largely retained (Table 2 and SI, section 5, S5). Radioactivity in the blood circulation was significantly higher for [^{125}I]-**2** compared to [^{125}I]-**4** (1 h p.i.; p = 0.01). As a consequence, accumulation in nontargeted organs and tissues was clearly higher after administration of radiofolate [^{125}I]-**2** compared to [^{125}I]-**4**. The liver accumulation of radioactivity after injection of [^{125}I]-**2** was high (>16% ID/g, 1 h p.i. and >2% ID/g, 4 h p.i.), but almost negligible in the case of [^{125}I]-**4** (<0.3% ID/g, 1 h p.i., p < 0.01, and <0.2% ID/g, 4 h p.i., p = 0.01). On the other hand, uptake in the gastrointestinal tract was comparable for both radiotracers (~4.5% ID/g, 1 h p.i.). With regard to uptake in the thyroid glands, large amounts of radioactivity (>1000% ID/g, 4 h p.i.) were found for [^{125}I]-**2**, whereas a more than 10-fold lower accumulation was observed in the case of [^{125}I]-**4**. Intraperitoneal administration of potassium iodide 1 h prior to administration of the radiotracer reduced the undesired uptake of iodide in the thyroid glands significantly ([^{125}I]-**2**: 13.74 ± 5.01% ID/g and [^{125}I]-**4**: 2.53 ± 0.39% ID/g, 4 h p.i.).

SPECT/CT Imaging and *Ex Vivo* Autoradiography. Figure 5 shows SPECT/CT images of mice after administration of the radiotracer [^{125}I]-**4**. The administration of potassium iodide effectively blocked the uptake of radioactivity in the thyroid gland (Figure 5A). After injection of PMX, renal retention of radioactivity was reduced to background levels (Figure 5B). SPECT/CT scans of a mouse that received both potassium iodide and PMX prior to the injection of [^{125}I]-**4** resulted in radioactivity uptake that was restricted to FR positive tumor xenografts, and only traces of radioactivity were observed in nontargeted organs and tissues (Figure 5C).

Images of *ex vivo* autoradiography studies are shown in Figure 6. The quantification of radioactivity uptake in tumor and kidney sections of the mouse that received PMX showed an uptake reduced to 56% (tumor) and 4% (kidney) of controls (SI, section 6).

DISCUSSION

Two different folic acid conjugates were synthesized and evaluated. In compound **1** tyrosine was conjugated to the γ-carboxyl group of the glutamate entity of folic acid, whereas in compound **3** tyrosine was conjugated to an azide-derivatized folic acid[27] via a "click" reaction, which resulted in a triazole-containing linker entity. Both folate conjugates (**1** and **3**) were readily radioiodinated using the Iodogen method. Separation from cold precursors gave high specific activities of [^{125}I]-**2** and [$^{125/131}$I]-**4**. The *in vitro* stability in human and murine plasma was high for both radiofolates. FR binding affinity and cell uptake were almost identical for both compounds and comparable to previously evaluated radiofolates.[24,28] *In vivo*, the ^{125}I-tyrosine-folate ([^{125}I]-**2**) was significantly instable. As a consequence, the high uptake of radioactivity was found in nontarget tissues and organs at early time points after injection of [^{125}I]-**2**. An increasingly high uptake of radioactivity was found in the thyroid gland which could be ascribed to the accumulation of free [^{125}I]-iodide. However, a significant reduction of radioactivity in the thyroid gland was achieved in mice that received a preinjection of potassium iodide. The low stability of [^{125}I]-**2** was further proven by the detection of significant amounts of free [^{125}I]-iodide in urine and blood samples (SI, Table S2). In contrast, free [^{125}I]-iodide was not detectable in blood samples after the injection of [^{125}I]-**4**, and only a low accumulation of radioactivity was found in the thyroid gland. The increased *in vivo* stability of [^{125}I]-**4** compared to [^{125}I]-**2** could be due to the "click" conjugation of the tyrosine entity, which may make the compound more resistant toward enzymatic attack.

Tumor uptake of the ^{125}I-tyrosine-folate ([^{125}I]-**2**) was significantly higher than for the ^{125}I-tyrosine-click-folate ([^{125}I]-**4**) at 1 and 4 h p.i. In the case of [^{125}I]-**2** it was not

Table 1. Biodistribution Data of [^{125}I]-2 and [^{125}I]-4 in KB Tumor-Bearing Nude Mice

	^{125}I-tyrosine-folate ([^{125}I]-**2**),[a] mean ± SD [%ID/g]				
dissection time	1 h p.i.	4 h p.i.	24 h p.i.	folic acid,[b] 4 h p.i.	KI,[c] 4 h p.i.
blood	3.00 ± 0.56	2.15 ± 0.42	0.09 ± 0.02	2.25 ± 1.00	2.71 ± 0.52
lung	2.66 ± 0.42	1.72 ± 0.25	0.11 ± 0.02	1.74 ± 0.68	2.04 ± 0.41
spleen	2.25 ± 0.58	1.60 ± 0.26	0.08 ± 0.03	1.72 ± 0.93	1.26 ± 0.15
kidneys	18.33 ± 2.47	9.80 ± 1.67	0.85 ± 0.06	1.79 ± 0.58	8.66 ± 1.86
stomach	9.44 ± 3.19	7.18 ± 0.62	0.20 ± 0.04	9.08 ± 5.49	4.44 ± 1.52
intestines	4.30 ± 1.01	1.65 ± 0.90	0.07 ± 0.01	2.25 ± 1.43	1.68 ± 0.48
liver	16.53 ± 1.20	2.74 ± 0.45	0.09 ± 0.01	0.83 ± 0.32	2.90 ± 0.63
salivary glands	13.32 ± 2.92	16.53 ± 3.42	1.36 ± 0.11	15.34 ± 9.09	4.02 ± 0.66
thyroid gland	261 ± 67	1059 ± 184	2830 ± 1272	868 ± 367	13.74 ± 5.01
muscle	1.45 ± 0.26	0.82 ± 0.30	0.02 ± 0.00	0.55 ± 0.24	0.53 ± 0.10
bone	1.59 ± 0.28	1.01 ± 0.24	0.03 ± 0.01	1.01 ± 0.53	0.98 ± 0.20
tumor	4.42 ± 0.66	3.43 ± 0.28	1.25 ± 0.18	1.65 ± 0.61	4.03 ± 0.22
tumor-to-blood	1.48 ± 0.18	1.65 ± 0.41	14.38 ± 3.66	0.74 ± 0.04	1.53 ± 0.30
tumor-to-liver	0.27 ± 0.04	1.28 ± 0.23	14.45 ± 1.88	1.98 ± 0.18	1.43 ± 0.24
tumor-to-kidney	0.24 ± 0.03	0.36 ± 0.06	1.47 ± 0.14	0.90 ± 0.09	0.48 ± 0.09
	^{125}I-tyrosine-click-folate ([^{125}I]-**4**),[a] mean ± SD [%ID/g]				
dissection time	control, 1 h p.i.	control, 4 h p.i.	control, 24 h p.i.	folic acid,[b] 4 h p.i.	KI,[c] 4 h p.i.
blood	0.10 ± 0.01	0.18 ± 0.15	0.01 ± 0.00	0.03 ± 0.00	0.08 ± 0.01
lung	0.59 ± 0.14	0.31 ± 0.09	0.05 ± 0.03	0.03 ± 0.00	0.23 ± 0.03
spleen	0.20 ± 0.02	0.14 ± 0.05	0.02 ± 0.00	0.02 ± 0.01	0.14 ± 0.02
kidneys	19.12 ± 0.58	16.44 ± 2.64	7.10 ± 1.44	0.08 ± 0.00	17.84 ± 2.60
stomach	0.94 ± 0.29	0.35 ± 0.08	0.12 ± 0.10	0.26 ± 0.31	1.01 ± 1.00
intestines	4.53 ± 1.77	1.24 ± 0.01	0.10 ± 0.01	0.46 ± 0.30	2.84 ± 1.16
liver	0.28 ± 0.08	0.15 ± 0.03	0.02 ± 0.00	0.02 ± 0.00	0.16 ± 0.03
salivary glands	6.11 ± 1.37	4.01 ± 1.31	0.42 ± 0.22	0.10 ± 0.04	3.49 ± 0.98
thyroid gland	8.36 ± 1.77	10.81 ± 4.99	47.59 ± 28.07	9.53 ± 8.10	2.47 ± 0.56
muscle	0.71 ± 0.13	0.32 ± 0.07	0.04 ± 0.04	0.01 ± 0.00	0.40 ± 0.04
bone	0.55 ± 0.05	0.23 ± 0.05	0.02 ± 0.01	0.02 ± 0.00	0.30 ± 0.01
tumor	2.36 ± 0.05	2.28 ± 0.46	1.92 ± 0.24	0.03 ± 0.01	2.53 ± 0.39
tumor-to-blood	23.21 ± 2.17	17.41 ± 9.66	286.75 ± 53.44	1.08 ± 0.47	30.93 ± 6.87
tumor-to-liver	8.73 ± 2.13	15.19 ± 3.99	84.82 ± 12.71	2.20 ± 0.96	15.78 ± 4.33
tumor-to-kidney	0.12 ± 0.00	0.14 ± 0.02	0.27 ± 0.05	0.41 ± 0.15	0.14 ± 0.02

[a] ~2.5 pmol/mouse. [b] FR blockade with folic acid (100 μg) i.v. coinjected. [c] Thyroid blockade with KI (4 mg) i.p. injected 1 h before the radiofolate.

Table 2. Biodistribution Data 4 h p.i. of [^{125}I]-4 in Combination with PMX in KB Tumor-Bearing Nude Mice

	^{125}I-tyrosine-click-folate ([^{125}I]-**4**),[a] mean ± SD [%ID/g]			
	control	PMX,[b] 400 μg	PMX,[b] 200 μg	PMX,[b] 100 μg
tumor	2.28 ± 0.46	1.55 ± 0.17	1.97 ± 0.26	2.97 ± 0.60
blood	0.18 ± 0.15	0.50 ± 0.75	0.07 ± 0.01	0.17 ± 0.12
liver	0.15 ± 0.03	0.88 ± 1.38	0.09 ± 0.01	0.18 ± 0.03
kidney	16.44 ± 2.64	1.08 ± 0.06	1.36 ± 0.26	5.17 ± 3.00
tumor-to-blood	17.41 ± 9.66	16.06 ± 11.85	29.45 ± 6.14	23.92 ± 12.54
tumor-to-liver	15.19 ± 3.99	13.50 ± 10.38	22.37 ± 4.27	16.43 ± 2.69
tumor-to-kidney	0.14 ± 0.02	1.44 ± 0.21	1.49 ± 0.35	0.72 ± 0.40

[a] ~2.5 pmol/mouse. [b] PMX was injected 1 h before the radiofolate.

possible to block the tumor uptake to background levels with excess folic acid. This indicates unspecific accumulation of radioactivity in the tumor, which can be ascribed to free [^{125}I]-iodide circulating in the blood. A relatively high accumulation of radioactivity was also found in the liver shortly after injection of [^{125}I]-**2** (>16% ID/g, 1 h p.i.) which might also be due to significant amounts of free [^{125}I]-iodide in the blood circulation. On the other hand, liver uptake of [^{125}I]-**4** was very low (<1% ID/g) compared to previously evaluated radiofolates.[28,29] Unfavorable accumulation of radioactivity in the intestinal tract early after injection was found with both radiofolates ([^{125}I]-**2** and [^{125}I]-**4**). This was possibly a result of their more lipophilic character compared to folate-based radiometal complexes (e.g. ^{111}In-DOTA-folate) as shown by determination of log *D* values ([^{125}I]-**2**: −2.87 ± 0.02 and [^{125}I]-**4**: −3.13 ± 0.07; SI).

At early time points after injection (1 h p.i.), the tumor-to-kidney ratios of radioactivity were low ([^{125}I]-**2**: 0.24 ± 0.03; [^{125}I]-**4**: 0.12 ± 0.00).[29] However, over time the tumor-to-kidney ratios increased ([^{125}I]-**2**: 1.47 ± 014; [^{125}I]-**4**: 0.27 ± 0.05; 24 h p.i.), which confirmed our hypothesis that partial deiodination may improve the tissue distribution. In addition,

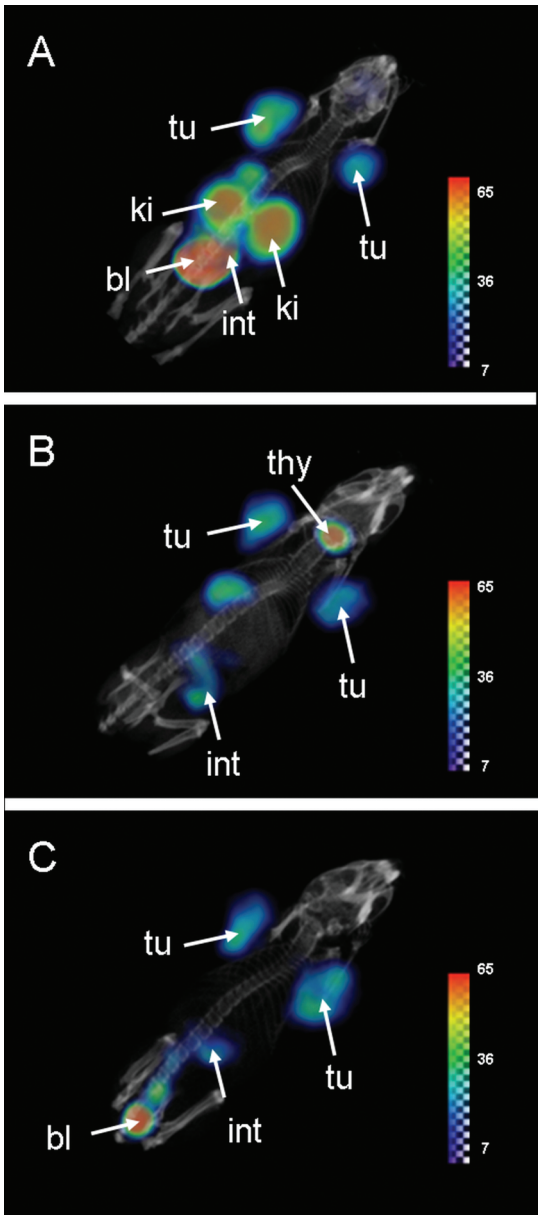

Figure 5. SPECT/CT images of KB tumor-bearing mice 24 h after injection of ^{125}I-tyrosine-click-folate ([^{125}I]-**4**): (A) with preinjected KI, (B) with preinjected PMX, and (C) with preinjected KI and PMX. (tu = tumor; ki = kidney; thy = thyroid gland; int = intestines; bl = urinary bladder).

as previously shown with other radiofolates, preinjection of PMX reduced kidney uptake in a dose-dependent manner without significantly affecting tumor accumulation.[14,30] Thus, predosing of PMX resulted in unprecedentedly high tumor-to-kidney ratios (4 h p.i.: ~1.5 and 24 h p.i.: ~3.0) of [^{125}I]-**4** (Table 2 and SI, section 5, Figure S4). These findings could be confirmed by *ex vivo* autoradiography (SI) and SPECT/CT imaging studies. However, it has to be critically acknowledged that the images were taken the day after injection of the radiofolate when unspecifically accumulated radiofolate had been excreted from the intestinal tract.

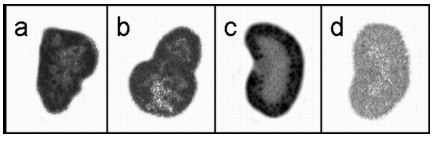

Figure 6. *Ex vivo* autoradiography of tissue sections after the injection of ^{125}I-tyrosine-click-folate [^{125}I]-**4** from KB tumors (A and B) and kidneys (C and D) from a control mouse (A and C) and a mouse that received preinjected PMX (B and D).

We were able to demonstrate *in vitro* that [^{131}I]-**4** reduced the viability of KB, IGROV-1, and SKOV-3 cells, but that the effect was not observed if FRs were blocked by incubation of these cells with excess folic acid. In addition, no inhibition of viability was observed in FR-negative PC-3 cells, which proved FR-mediated cytotoxicity. The determination of the radioactivity concentration of [^{131}I]-**4** necessary to reduce cell viability to 50% of untreated control cells showed that KB cells were more sensitive to radiofolate treatment than IGROV-1 and SKOV-3 cells. These findings are in agreement with the lower FR-expression levels on IGROV-1 and SKOV-3 cells compared to KB cells which express FRs at very high levels.[1,19,20] Recently, Bischof et al. demonstrated that PMX displayed radiosensitizing effects in combination with external radiation *in vitro*.[31,32] In the present study it could be shown that the application of PMX in combination with [^{131}I]-**4** enhanced the inhibitory effect on FR positive tumor cell viability. It is likely that the coapplication of therapeutic radiofolates and PMX could also enhance FR targeted radionuclide therapy *in vivo* similar to the application of 5-fluorouracil, which has been applied in the clinics in combination with peptide and antibody-based targeted radionuclide therapies.[33−35]

In this study we were able to demonstrate that radioiodinated folate conjugates would be favorable with respect to a therapeutic application because partial *in vivo* deiodination results in low kidney retention of radioactivity over time. On the other hand, we also experienced that too low stability as is the case for [^{125}I]-**2** would be less advantageous as it results in unspecific uptake of radioactivity in nontargeted tissues. With respect to the improved tracer design, finding an optimal balance between sufficient plasma stability and partial *in vivo* deiodination of the radiofolate would be desirable. Nevertheless, we believe that radioiodinated folate conjugates provide a suitable concept for FR targeted radionuclide therapy, particularly in combination with PMX, which we proved for the first time results in an enhanced anticancer effect *in vitro*.

■ ASSOCIATED CONTENT

Supporting Information

Organic syntheses and radioiodination, octanol/PBS distribution coefficient, investigation of metabolic stability using liver microsomes, metabolite studies, biodistribution of [^{125}I]-**4** in combination with pemetrexed, and *ex vivo* autoradiography. This material is available free of charge via the Internet at http://pubs.acs.org.

■ AUTHOR INFORMATION

Corresponding Author

*Paul Scherrer Institute, Center for Radiopharmaceutical Sciences ETH-PSI-USZ 5232, Villigen-PSI, Switzerland. E-mail: cristina.mueller@psi.ch. Phone: +41-56-310 44 54; fax: +41-56-310 28 49.

Notes

The authors declare no competing financial interest.

■ ACKNOWLEDGMENTS

We thank Nadja Romano, Alain Blanc, and Kurt Hauenstein for technical assistance. This project was supported by the Swiss National Science Foundation (Ambizione PZ00P3_121772) and COST (Action BM0607).

■ REFERENCES

(1) Weitman, S. D.; Lark, R. H.; Coney, L. R.; Fort, D. W.; Frasca, V.; Zurawski, V. R.; Kamen, B. A. Distribution of the folate receptor GP38 in normal and malignant cell lines and tissues. *Cancer Res.* **1992**, *52* (12), 3396−3401.

(2) Antony, A. C. Folate receptors. *Ann. Rev. Nutr.* **1996**, *16*, 501−521.

(3) Parker, N.; Turk, M. J.; Westrick, E.; Lewis, J. D.; Low, P. S.; Leamon, C. P. Folate receptor expression in carcinomas and normal tissues determined by a quantitative radioligand binding assay. *Anal. Biochem.* **2005**, *338* (2), 284−293.

(4) Low, P. S.; Henne, W. A.; Doorneweerd, D. D. Discovery and development of folic-acid-based receptor targeting for imaging and therapy of cancer and inflammatory diseases. *Acc. Chem. Res.* **2008**, *41* (1), 120−9.

(5) Ke, C. Y.; Mathias, C. J.; Green, M. A. Folate-receptor-targeted radionuclide imaging agents. *Adv. Drug Delivery Rev.* **2004**, *56* (8), 1143−1160.

(6) Sega, E. I.; Low, P. S. Tumor detection using folate receptor-targeted imaging agents. *Cancer Metastasis Rev.* **2008**, *27* (4), 655−64.

(7) Müller, C.; Schibli, R. Folic acid conjugates for nuclear imaging of folate receptor-positive cancer. *J. Nucl. Med.* **2011**, *52* (1), 1−4.

(8) Holm, J.; Hansen, S. I.; Hoiermadsen, M.; Bostad, L. A high-affinity folate binding-protein in proximal tubule cells of human kidney. *Kidney Int.* **1992**, *41* (1), 50−55.

(9) Birn, H.; Spiegelstein, O.; Christensen, E. I.; Finnell, R. H. Renal tubular reabsorption of folate mediated by folate binding protein 1. *J. Am. Soc. Nephrol.* **2005**, *16* (3), 608−615.

(10) Sandoval, R. M.; Kennedy, M. D.; Low, P. S.; Molitoris, B. A. Uptake and trafficking of fluorescent conjugates of folic acid in intact kidney determined using intravital two-photon microscopy. *Am. J. Physiol. Cell Physiol.* **2004**, *287* (2), C517−C526.

(11) Müller, C.; Vlahov, I. R.; Santhapuram, H. K.; Leamon, C. P.; Schibli, R. Tumor targeting using ^{67}Ga-DOTA-Bz-folate - investigations of methods to improve the tissue distribution of radiofolates. *Nucl. Med. Biol.* **2011**, *38* (5), 715−23.

(12) Müller, C.; Brühlmeier, M.; Schubiger, A. P.; Schibli, R. Effects of antifolate drugs on the cellular uptake of radiofolates in vitro and in vivo. *J. Nucl. Med.* **2006**, *47* (12), 2057−2064.

(13) Müller, C.; Schibli, R.; Krenning, E. P.; de Jong, M. Pemetrexed improves tumor selectivity of ^{111}In-DTPA-folate in mice with folate receptor-positive ovarian cancer. *J. Nucl. Med.* **2008**, *49* (4), 623−9.

(14) Müller, C.; Reddy, J. A.; Leamon, C. P.; Schibli, R. Effects of the Antifolates Pemetrexed and CB3717 on the Tissue Distribution of Tc-99m-EC20 in Xenografted and Syngeneic Tumor-Bearing Mice. *Mol. Pharmaceutics* **2010**, *7* (2), 597−604.

(15) Tarli, L.; Balza, E.; Viti, F.; Borsi, L.; Castellani, P.; Berndorff, D.; Dinkelborg, L.; Neri, D.; Zardi, L. A high-affinity human antibody that targets tumoral blood vessels. *Blood* **1999**, *94* (1), 192−8.

(16) Berndorff, D.; Borkowski, S.; Moosmayer, D.; Viti, F.; Müller-Tiemann, B.; Sieger, S.; Friebe, M.; Hilger, C. S.; Zardi, L.; Neri, D.; Dinkelborg, L. M. Imaging of tumor angiogenesis using ^{99m}Tc-labeled human recombinant anti-ED-B fibronectin antibody fragments. *J. Nucl. Med.* **2006**, *47* (10), 1707−16.

(17) Krummeich, C.; Holschbach, M.; Stocklin, G. Direct n.c.a. electrophilic radioiodination of tyrosine analogues; their in vivo stability and brain-uptake in mice. *Appl. Radiat. Isot.* **1994**, *45* (9), 929−35.

(18) Arlt, M. J.; Novak-Hofer, I.; Gast, D.; Gschwend, V.; Moldenhauer, G.; Grunberg, J.; Honer, M.; Schubiger, P. A.; Altevogt, P.; Kruger, A. Efficient inhibition of intra-peritoneal tumor growth and dissemination of human ovarian carcinoma cells in nude mice by anti-L1-cell adhesion molecule monoclonal antibody treatment. *Cancer Res.* **2006**, *66* (2), 936−43.

(19) Ke, C. Y.; Mathias, C. J.; Green, M. A. The folate receptor as a molecular target for tumor-selective radionuclide delivery. *Nucl. Med. Biol.* **2003**, *30* (8), 811−817.

(20) Garin-Chesa, P.; Campbell, I.; Saigo, P. E.; Lewis, J. L.; Old, L. J.; Rettig, W. J. Trophoblast and ovarian cancer antigen LK26 - sensitivity and specificity in immunopathology and molecular identification as a folate-binding protein. *Am. J. Pathol.* **1993**, *142* (2), 557−567.

(21) Hattori, Y.; Maitani, Y. Folate-linked nanoparticle-mediated suicide gene therapy in human prostate cancer and nasopharyngeal cancer with herpes simplex virus thymidine kinase. *Cancer Gene Ther.* **2005**, *12* (10), 796−809.

(22) Ladino, C. A.; Chari, R. V. J.; Bourret, L. A.; Kedersha, N. L.; Goldmacher, V. S. Folate-maytansinoids: target-selective drugs of low molecular weight. *Int. J. Cancer* **1997**, *73* (6), 859−864.

(23) Mathias, C. J.; Wang, S.; Lee, R. J.; Waters, D. J.; Low, P. S.; Green, M. A. Tumor-selective radiopharmaceutical targeting via receptor-mediated endocytosis of gallium-67-deferoxamine-folate. *J. Nucl. Med.* **1996**, *37* (6), 1003−1008.

(24) Müller, C.; Hohn, A.; Schubiger, P. A.; Schibli, R. Preclinical evaluation of novel organometallic ^{99m}Tc-folate and ^{99m}Tc-pteroate radiotracers for folate receptor-positive tumour targeting. *Eur J. Nucl. Med. Mol. Imaging* **2006**, *33* (9), 1007−1016.

(25) Leamon, C. P.; Parker, M. A.; Vlahov, I. R.; Xu, L. C.; Reddy, J. A.; Vetzel, M.; Douglas, N. Synthesis and biological evaluation of EC20: a new folate-derived, ^{99m}Tc-based radiopharmaceutical. *Bioconjugate Chem.* **2002**, *13* (6), 1200−1210.

(26) Reddy, J. A.; Xu, L. C.; Parker, N.; Vetzel, M.; Leamon, C. P. Preclinical evaluation of ^{99m}Tc-EC20 for imaging folate receptor-positive tumors. *J. Nucl. Med.* **2004**, *45* (5), 857−866.

(27) Mindt, T. L.; Müller, C.; Melis, M.; de Jong, M.; Schibli, R. "Click-to-chelate": in vitro and in vivo comparison of a ^{99m}Tc(CO)$_3$-labeled N(tau)-histidine folate derivative with its isostructural, clicked 1,2,3-triazole analogue. *Bioconjugate Chem.* **2008**, *19* (8), 1689−95.

(28) Müller, C.; Forrer, F.; Schibli, R.; Krenning, E. P.; de Jong, M. SPECT study of folate receptor-positive malignant and normal tissues in mice using a novel ^{99m}Tc-radiofolate. *J. Nucl. Med.* **2008**, *49* (2), 310−317.

(29) Müller, C.; Mindt, T. L.; de Jong, M.; Schibli, R. Evaluation of a novel radiofolate in tumour-bearing mice: promising prospects for folate-based radionuclide therapy. *Eur. J. Nucl. Med. Mol. Imaging* **2009**, *36* (6), 938−46.

(30) Müller, C.; Schibli, R.; Forrer, F.; Krenning, E. P.; de Jong, M. Dose-dependent effects of (anti)folate preinjection on ^{99m}Tc-radiofolate uptake in tumors and kidneys. *Nucl. Med. Biol.* **2007**, *34* (6), 603−8.

(31) Bischof, M.; Weber, K. J.; Blatter, J.; Wannenmacher, M.; Latz, D. Interaction of pemetrexed disodium (ALIMTA, multitargeted antifolate) and irradiation in vitro. *Int. J. Radiat. Oncol. Biol. Phys.* **2002**, *52* (5), 1381−8.

(32) Bischof, M.; Huber, P.; Stoffregen, C.; Wannenmacher, M.; Weber, K. J. Radiosensitization by pemetrexed of human colon carcinoma cells in different cell cycle phases. *Int. J. Radiat. Oncol. Biol. Phys.* **2003**, *57* (1), 289−92.

(33) Wong, J. Y.; Shibata, S.; Williams, L. E.; Kwok, C. S.; Liu, A.; Chu, D. Z.; Yamauchi, D. M.; Wilczynski, S.; Ikle, D. N.; Wu, A. M.; Yazaki, P. J.; Shively, J. E.; Doroshow, J. H.; Raubitschek, A. A. A Phase I trial of ^{90}Y-anti-carcinoembryonic antigen chimeric T84.66 radioimmunotherapy with 5-fluorouracil in patients with metastatic colorectal cancer. *Clin. Cancer Res.* **2003**, *9* (16 Pt 1), 5842−52.

(34) van Essen, M.; Krenning, E. P.; Kam, B. L.; de Herder, W. W.; van Aken, M. O.; Kwekkeboom, D. J. Report on short-term side effects of treatments with ^{177}Lu-octreotate in combination with capecitabine in seven patients with gastroenteropancreatic neuroendocrine tumours. *Eur. J. Nucl. Med. Mol. Imaging* **2008**, *35* (4), 743−8.

(35) Claringbold, P. G.; Brayshaw, P. A.; Price, R. A.; Turner, J. H. Phase II study of radiopeptide ^{177}Lu-octreotate and capecitabine

therapy of progressive disseminated neuroendocrine tumours. *Eur. J. Nucl. Med. Mol. Imaging* **2011**, *38* (2), 302−11.